Paper accepted for presentation at 2009 IEEE Bucharest Power Tech Conference, June 28th - July 2nd, Bucharest, Romania

Risk-Based TTC Calculation of a Power System with Renewable Energy Resources

Nattawut Paensuwan and Akihiko Yokoyama, *Member, IEEE*

***Abstract*—Recently, the electric power utilities worldwide have been moving toward the utilization of renewable energy resources because of their sustainability, environmental friendliness, and as promising low-cost energies for the future electricity production. Although a number of appealing advantages are expected, a large penetration of generation from renewable energy resources may cause some undesirable impact on system security and reliability due to the uncertainty of their generation output. Therefore, the power system analysis should be able to cope with and examine the influences resulting from the presence of this sector. In this paper, the influences on the TTC are investigated via the risk and monetary loss. The uncertainty of the forecast demand and the generation output from renewable energy resources is integrated into the calculation by a probabilistic method, Monte Carlo simulation. Furthermore, a partition technique for the Monte Carlo simulation is proposed for the speed enhancement.**

***Index Terms*—Renewable energy resources, total transfer capability.**

I. Introduction

In recent years, a rapid penetration of generation from renewable energy resources, e.g. wind and solar energies, has been witnessed around the world. The main incentives of this rapid growth are due to rising environmental concerns, and cost escalation associated with conventional energies used for electricity production. In addition, a significant amount of installed capacity can also be expected within the near future. For instance, Japan Renewable Energy Policy Platform (JREPP) was launched with the projected 18% electricity substitution by solar power in 2050 [1]. Although the application of wind and photovoltaic (PV) technologies offers a great appeal and several advantages, a large penetration may cause unfavorable influences on the system security and reliability [2]. Consequently, this poses a need for an extensive research on evaluating the impact of this rapidly growing sector to ensure a secure and reliable system operation.

This paper primarily concentrates on the TTC calculation of an electric power system with wind and photovoltaic (PV) power generations. Several literatures on the transfer capability calculation with wind power generation have been reported in [3], [4], [5]. As is known, wind and PV power generations have highly fluctuating generation outputs. These outputs are uncertain and vary on hourly or daily basis depending on the weather condition or wind speed. With this regard, a probabilistic approach, rather than a deterministic approach, is more appropriate in recognizing and coping with such a stochastic nature of these outputs.

An endeavor has been made to develop the models representing the renewable energy resources for the power system analysis. The wind power generation system can be represented simply by a PQ model [3], [6] or by an RX model with the use of a steady-state model of an induction generator [4]. In contrast, the PV power generation system is commonly represented by a PQ model [7]. This paper proposes the PX model for the wind power generation system, which is simple to be incorporated into the TTC calculation. In addition, a partitioned Monte Carlo simulation, a modified version of a typical Monte Carlo simulation with some partition technique, is presented to improve the computational speed.

This paper is organized in the following sequences. In Section II, the risk-based TTC calculation and the MTC calculation by OPF are explained. In Section III, the wind power generation system modeling is presented. In Section IV, the photovoltaic (PV) power generation system modeling is described. Section V summarizes the proposed partitioned Monte Carlo simulation, monetary loss calculation, and the overall procedures of the proposed TTC calculation. Numerical examples and results of the proposed method applied to the modified IEEE 30-bus system are presented in Section VI. Finally, the conclusions are provided in Section VII.

II. TTC Calculation

A. TTC Definition and MTC Calculation

According to NERC, TTC was defined as the maximum of power that can be transferred in a reliable manner between a pair of defined source and sink locations in the interconnected system while meeting all of a specific set of defined pre- and post- contingency system conditions [8].

Generally, to find the TTC, another closely related term, Maximum Transfer Capability (MTC), has to be determined for a given set of various system scenarios. The MTC represents the maximum transferable electric power under a given system scenario. A number of methods have been developed for the MTC calculation; Repeated Power Flow (RPF) [9], Continuation Power Flow (CPF) [10], Two-step method [11], and Optimal Power Flow (OPF) [12]. The first three methods are based on solving a power flow problem, while the last is based on solving an optimization problem. This paper employs the OPF to solve for the MTC. The formulation of the OPF is summarized in the following.

Consider an area-to-area TTC in which the power is transferred from a source area to a sink area as depicted in Fig. 1.

Nattawut Paensuwan is with the Department of Electrical Engineering, the University of Tokyo, Tokyo, 113-8656 Japan (e-mail: pnattawut@syl.t.u-tokyo.ac.jp).

Akihiko Yokoyama is with the Department of Advanced Energy, the University of Tokyo, Chiba, 277-8561 Japan (e-mail: yokoyama@syl.t.u-tokyo.ac.jp).

978-1-4244-2235-7/09/$25.00 ©2009 IEEE

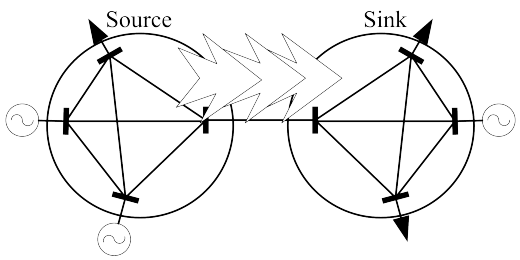

Fig. 1. Representation of an area-to-area TTC.

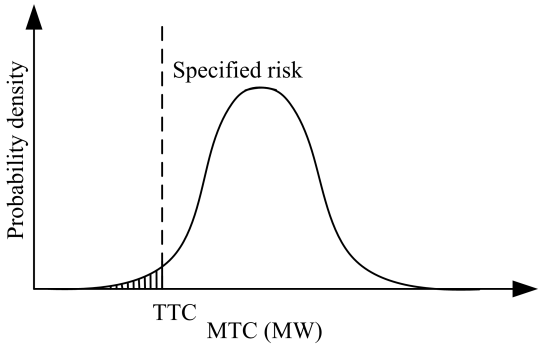

Fig. 2. PDF of the MTC with the specified risk and corresponding TTC.

This additional transfer is then delivered to the sink buses in the sink area, which is represented by a scalar λ. Therefore, maximizing the transfer is equivalent to maximizing the λ.

The constraints in the OPF are composed of equality constraints which account for the power balance equations, and inequality constraints which account for the system security limits. Typically, the system security limits which restricts the ability of a system to transfer electric power are as follows.

1) Voltage magnitude limit
2) Generation capacity limit
3) Transmission line thermal limit
4) Transient stability limit
5) Voltage stability limit

In this paper, the transient stability limit is taken into account by a widely used static criterion, the bus voltage angle limit, i.e. $-45^\circ \leq \delta \leq 45^\circ$. For the sake of simplicity, the voltage stability limit is not considered. With the additional electric power transferred to the sink buses, the active and reactive demands at the sink buses are modified as follows:

$$P_{Di} = P_{Di}^0 + \lambda \cos(\psi_i^0) \tag{1}$$

$$Q_{Di} = Q_{Di}^0 + \lambda \sin(\psi_i^0) \tag{2}$$

where P_{Di}, Q_{Di} are active and reactive demands at the sink bus i; P_{Di}^0, Q_{Di}^0 are base-case active and reactive demands at the sink bus i; λ is a load parameter; ψ_i^0 is the base-case power factor angle of the sink bus i. The optimization problem can be formulated in a general form as:

$$\left.\begin{array}{l} \max \quad \lambda \\ \text{s.t.} \\ G(x,\lambda) = 0 \\ H(x,\lambda) \leq 0 \end{array}\right\} \tag{3}$$

where x is a vector of system control and state variables, $G(x,\lambda)$ are a set of equality constraints, and $H(x,\lambda)$ are a set of inequality constraints respectively. Once the maximum λ is solved, the MTC is computed from

$$MTC = \sum_{i=1}^{N_{Sink}} \left(P_{Di}^0 + \lambda_{max} \cos(\psi_i^0)\right) \tag{4}$$

where N_{Sink} is the number of sink buses.

B. Risk-Based TTC Selection

The selection of the TTC is based on the risk concept proposed in [13], [14]. To apply the risk concept, the probability density function or PDF of the MTC is required. In this paper, it is obtained from the Monte Carlo simulation. According to the PDF of the MTC, the risk refers to the accumulated probability of the cases whose MTC's are smaller than the selected TTC as depicted in Fig. 2. It should be noted that the risk here is mainly associated with the additional transfer power above the base-case condition not the base-case condition itself. Although the system has sufficient generation capacity, it sometimes cannot deliver the electric power to the sink locations at the promised volume, i.e. TTC, due to the outages. Such circumstance is the risk considered in this paper.

III. Wind Power Generation System Modeling

The conversion of mechanical power of the wind turbine into electrical power is usually accomplished by an induction generator. In many literatures, the induction generator is commonly modeled as a PQ bus. The active power generation is assumed to be known with a given power factor from which the reactive power is calculated. The accuracy can be improved by taking into account the steady-state model of an induction generator shown in Fig. 3 [15].

In this paper, the PX model of an induction generator is proposed in which the generated active power is known by means of the forecasting process, and the consumed reactive power is calculated as a function of the induction generator's parameters, terminal voltage, and rotor slip.

In Fig. 3, P_e is the electrical active power injected to the system; P_m is the mechanical input power from the wind turbine; V is the terminal voltage; R_s, R_r are the stator and rotor resistances; X_s, X_r are the stator and rotor reactances; X_m is the magnetizing reactance; s is the slip. Simplifying the model in Fig. 3, gives an equivalent model in Fig. 4.

The equivalent resistance and reactance are written in terms of the slip as follows:

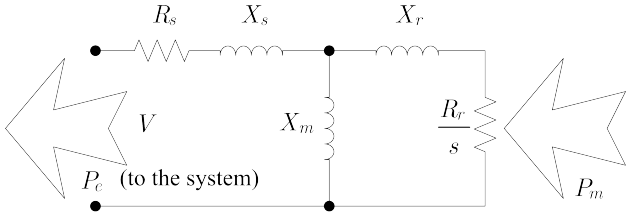

Fig. 3. Steady-state model of an induction generator.

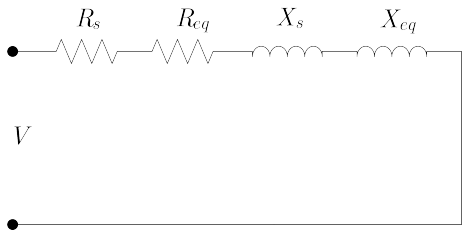

Fig. 4. Equivalent model of an induction generator.

$$R_{eq}(s) = \frac{\frac{R_r X_m^2}{s}}{\frac{R_r^2}{s} + (X_m + X_r)^2} \tag{5}$$

$$X_{eq}(s) = \frac{\frac{R_r^2 X_m}{s} + X_m X_r (X_m + X_r)}{\frac{R_r^2}{s} + (X_m + X_r)^2} \tag{6}$$

Let $R(s) = R_s + R_{eq}(s)$ and $X(s) = X_s + X_{eq}(s)$, the active power generated and the reactive power consumed by the induction generator can be written as:

$$P_{IG}(V, s) = \frac{V^2}{R^2(s) + X^2(s)} R(s) \tag{7}$$

$$Q_{IG}(V, s) = \frac{V^2}{R^2(s) + X^2(s)} X(s) \tag{8}$$

Note that, the active power term in (7) is negative since the rotor slip is negative. In other words, it can be conceived as negative load.

Incorporating this PX model into the power flow calculation introduces a new state variable, i.e. the rotor slip. Therefore, another equation is required to enforce P_{IG} to its specified value. The power balance equations of bus i connected to the wind power generation system are modified as follows:

$$f_{Pi} = F_{Pi}(\delta, V) - (P_{IGi}^{spec} - P_{Di}) = 0 \tag{9}$$

$$f_{Qi} = F_{Qi}(\delta, V) - (-Q_{Di} - Q_{IGi}(V_i, s_i)) = 0 \tag{10}$$

where

$$F_{Pi}(\delta, V) = \sum_{j=1}^{N} V_i V_j (G_{ij} \cos \delta_{ij} + B_{ij} \sin \delta_{ij})$$

$$F_{Qi}(\delta, V) = \sum_{j=1}^{N} V_i V_j (G_{ij} \sin \delta_{ij} - B_{ij} \cos \delta_{ij})$$

Here G_{ij} and B_{ij} are the real and imaginary parts of the ij^{th} element in the admittance matrix; V_i and V_j are the voltage magnitudes at bus i and j respectively; δ_{ij} is the voltage angle difference between bus i and j; N is the number of buses. To enforce P_{IGi} to its specified value P_{IGi}^{spec}, the following equation is added.

$$f_{P_{IG}i}(V_i, s_i) = -P_{IGi}(V_i, s_i) - P_{IGi}^{spec} = 0 \tag{11}$$

Then, the augmented power flow problem can be formulated as follows:

$$\begin{bmatrix} \frac{\partial f_P}{\partial \delta} & \frac{\partial f_P}{\partial V} & \frac{\partial f_P}{\partial s} \\ \frac{\partial f_Q}{\partial \delta} & \frac{\partial f_Q}{\partial V} & \frac{\partial f_Q}{\partial s} \\ \frac{\partial f_{P_{IG}}}{\partial \delta} & \frac{\partial f_{P_{IG}}}{\partial V} & \frac{\partial f_{P_{IG}}}{\partial s} \end{bmatrix} \begin{bmatrix} \Delta\delta \\ \Delta V \\ \Delta s \end{bmatrix} = \begin{bmatrix} \Delta f_P \\ \Delta f_Q \\ \Delta f_{P_{IG}} \end{bmatrix} \tag{12}$$

The power flow calculation is performed prior to the OPF calculation at each given system scenario sampled from the Monte Carlo simulation to adjust the generation according to the system parameters' change from the base-case condition.

With the proposed PX model, the induction generator can be incorporated into the power flow analysis. Furthermore, this PX model can also be easily incorporated into the OPF. The OPF formulation for the MTC calculation with induction generators is similar to (3) but with a new set of equality constraints to account for (11). In addition, using the PX model, the reactive power can be computed directly. On the contrary, the PQ model computes the reactive power simply from the specified power factor which may not be kept at all time due to the capacitor's capacity limit. This reactive power demand of the induction generator generally causes the terminal voltage to drop, hence restricting the transfer capability. As a result, an inaccurate model accounting for the reactive power results in inaccurate TTC value.

IV. PV Power Generation System Modeling

The photovoltaic (PV) power technology uses semiconductor cells to convert solar energy to electrical energy. In the past, the PV applications have been limited to remote locations not connected to the utility grid or isolated regions. With the declining price and improvements in manufacturing, this sector is expected to grow and play a significant role in the future electricity production. The United States, Japan, India, China, and other countries have launched new programs to expand the installed capacity within the near future [16].

As is known, the generation output of the PV system strongly depends on the weather condition, sunny or overcast. Therefore, the output of the PV system is very uncertain. A considerable deviation from the forecast value is possible in an actual interested time interval. Normally, if the radiation intensity is known, the generation output of the PV power generation system can be predicted. Nonetheless, the accurate prediction of radiation intensity for a day in advance is relatively difficult.

In this paper, the PV power generation system is modeled as a PQ bus operating at a unity power factor. The deviation of its generation output from the scheduled value is represented through the normal probability distribution.

V. Proposed Method

A. Partitioned Monte Carlo Simulation

The probabilistic method used in this paper is a well known Monte Carlo simulation. The Monte Carlo simulation is a statistical assessment based on a sampling technique using a random number. This technique has been well reported

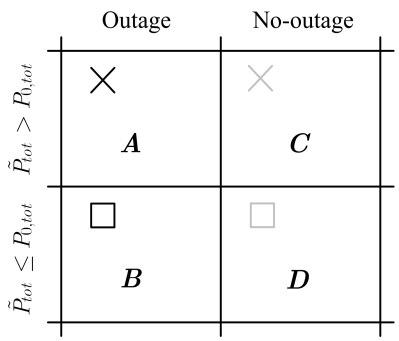

Fig. 5. Classification of the system cases.

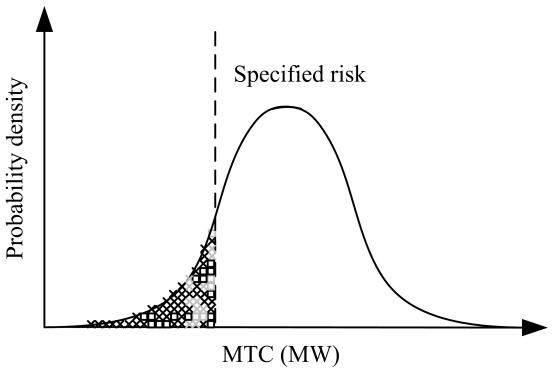

Fig. 6. Distribution of the MTC's from each partitioned set in the risk area.

in many TTC literatures. A full Monte Carlo simulation usually requires a sufficiently large sample size to ensure the convergence; as a result, it is time-consuming. In this paper, a partitioned Monte Carlo simulation is proposed. Referring to the risk-based TTC selection described in Section II, it can be seen that not all the system cases cause the risk. If there is no outage, the system is less likely to cause the risk, i.e., the system can transfer a large amount of electric power. On the other hand, if an outage occurs, the system configuration changes due to the corrective actions; consequently, the system may lose its ability to transfer electric power. In other words, the MTC's of the outage cases are generally smaller than those of the no-outage cases. In brief, to obtain the risk-based TTC, it is not necessary to compute the MTC of all system cases, only those leading to the risk are sufficient. Based on this concept, the system cases will be partitioned into 2 main groups; risk-related and merely-risk-related cases respectively.

The criteria for classifying the system cases are based on the following characteristics. In general, the ability of a system to transfer electric power is degraded when there occurs an outage or the system demand is large. Consequently, the risk-related cases mainly consist of the outage cases and the system cases in which the total sampled demand is larger than the total base-case demand. Considering only the above partitioned cases, a significant number of the OPF calculations in the Monte Carlo simulation can be avoided; as a result, greatly saving the computational time.

The classification of the system cases can be illustrated by the diagram as shown in Fig. 5. In Fig. 5, $\tilde{P}_{tot}$ is the total sampled demand; $P_{0,tot}$ is the total base-case demand; A is a set of outage cases with $\tilde{P}_{tot} > P_{0,tot}$; B is a set of outage cases with $\tilde{P}_{tot} \leq P_{0,tot}$; C is a set of no-outage cases with $\tilde{P}_{tot} > P_{0,tot}$; and D is a set of no-outage cases with $\tilde{P}_{tot} \leq P_{0,tot}$. The distribution of the MTC's from each set is depicted in Fig. 6.

Shown in Fig. 6, the risk area is composed of the MTC's mostly from a set A denoted by a black cross, a set B denoted by a black square, and a set C denoted by a gray cross. It is interesting to note that for a system with a large number of outage cases, only a set $A \cup B$ may be sufficient to cover the risk area within a certain degree of accuracy.

Importantly, the readers should note that the main objective of the proposed partitioned Monte Carlo simulation is to save the computational time by performing only the necessary calculations. Therefore, the proposed partitioned Monte Carlo simulation is just an approximation with some knowledge to avoid the unnecessary calculations. Inevitably, some precision may be traded off for the reduction of the computational time.

B. Monetary Loss Evaluation

As mentioned in Section II, the risk occurs when the actual amount of the transfer is smaller than the specified one. This circumstance results in interrupted energy to end-users. The monetary impact from the interruption can be described by an interrupted energy cost [17]. The risk function can be expressed as follows:

$$R(x) = \sum_{x=-\infty}^{TTC} IEAR(TTC - x) f(x) \Delta x \qquad (13)$$

where $IEAR$ is an interrupted energy assessment rate (in \$/MWh); x is the actual amount of the transferable electric power; $f(x)$ is the PDF of the MTC. It should be noted that the risk function in (13) depends on the probabilistic nature of the transferred power.

C. Proposed TTC Calculation

This subsection summarizes the overall procedures of the proposed TTC calculation by a partitioned Monte Carlo simulation. It comprises three main parts; (1) sampling and partitioning, (2) Monte Carlo simulation, and (3) TTC selection and monetary loss calculation. The procedures of the proposed method are summarized in Fig 7. The parameters to be sampled in the Monte Carlo simulation are as follows.

1) System case:
   The system case can be sampled using a state sampling technique [18]. The availability of the system component is assumed a two-state Markov model with the failure and repair transition rates. These data are obtained from the historical reliability data, normally well collected by the utilities.
2) System demand:
   The system demand in the TTC calculation is the forecast demand. In this paper, the forecast demand is assumed to have a normal distribution with a specified

standard deviation. As a result, the demand can be sampled from

$$x = \mu_x + \sigma_x Z \tag{14}$$

where x is the sampled demand; μ_x is the forecast demand; σ_x is the standard deviation of the demand; Z is a normal distributed random number.

3) Generation outputs from renewable energy resources: Similarly, the generation outputs from renewable energy resources are modeled as the forecast value plus some error specified in terms of the standard deviation. As a result, they can also be sampled using (14).

VI. Numerical Examples

A. Studied System

The modified IEEE 30-bus system has been used for the demonstration with the single-line diagram shown in Fig. 8. The system consists of 6 conventional generators with the total generation capacity of 335 MW, 17 wind power generation units located at buses#3, 4, 7, 8, 11, 17, 19, and 26 (some buses have multiple units); 9 PV power generation units located at buses#14, 15, 16, 18, 19, 20, 23, 29, and 30. The system is divided into 2 areas; source and sink areas. The forecast generation outputs from wind and PV power generation systems are 1.0, 1.2 MW and 4 MW respectively with the total of 54 MW. For wind power generation systems, the reactive power is compensated from a 400 kVAr capacitor bank connected at the system site. The total system demand is 189.2 MW.

B. Parameter Set-Up

As is known, Monte Carlo simulation creates a fluctuating convergence process. The error bound decreases as the number of samples increases. The commonly used stopping criteria for the Monte Carlo simulation are the coefficient of variation and the number of samples. In this paper, the number of samples of 5000 is used as the stopping criterion which is found to be sufficient for the convergence of simulation process.

The contingencies considered here are only three-phase faults on transmission lines up to N-2 contingencies. The FOR of each transmission line is 0.01. The total base-case generation output from the wind power generation systems is 18 MW and that from the PV power generation systems is 36 MW.The base-case demand in the sink area is 56.2 MW. For the monetary loss evaluation, the $IEAR$ is 500$/MWh. All calculations are run on a Pentium IV 3.4 GHz 1 GB RAM personal computer using a program developed in the MATLAB environment.

C. Study Cases

In this paper, two aspects are of interest. The first one is the impact of the uncertainty of the forecast demand and generation outputs from renewable energy resources. The other is the reduction of the computational time by using the partitioned Monte Carlo simulation. Seven comparative study cases are conducted, each of which is with the different degree of uncertainty. The summary of the study cases are listed in Table I.

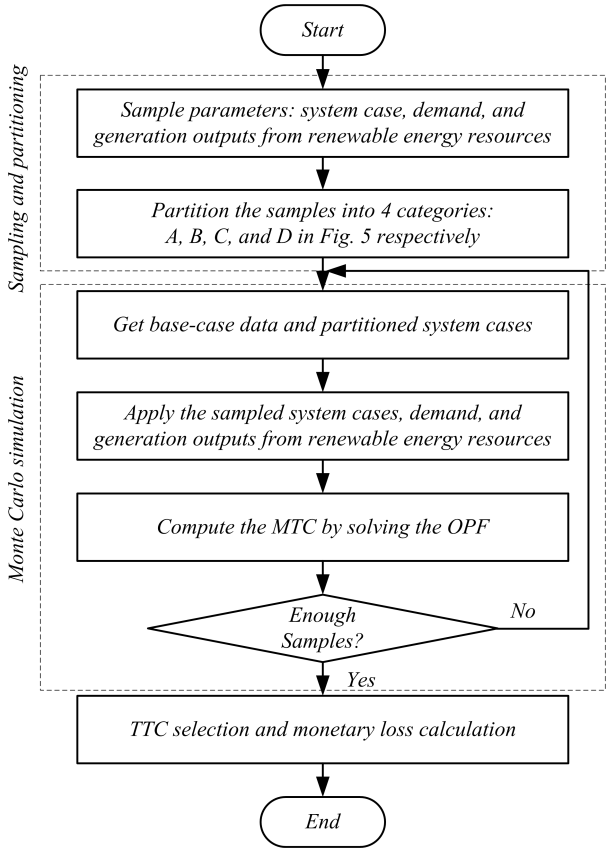

Fig. 7. Flowchart of the proposed method.

TABLE I
Summary of the Study Cases

Case	$\sigma_{PD}(\%)$	$\sigma_{PW}(\%)$	$\sigma_{PPV}(\%)$
1	0	0	0
2a	0	30	30
2b	0	40	40
2c	0	50	50
3a	10	30	30
3b	10	40	40
3c	10	50	50

In Table I, σ_{PD}, σ_{PW}, σ_{PPV} are the standard deviations of the forecast demand, forecast generation output from a wind power generation system, and forecast generation output from a PV power generation system respectively. These standard deviations are defined in percent of their forecast values. Case 1 is the base-case TTC without any uncertainty of the forecast parameters except that of the system state. Case 2a, 2b, and 2c consider only the forecast generation output uncertainty. The uncertainty degree increases from 30% to 50%. Similarly, Case 3a, 3b, and 3c consider both forecast generation output and forecast demand uncertainty. The impacts of the uncertainty of the forecast demand and generation outputs from renewable energy resources will be expressed in terms of risk and monetary loss as discussed in Section V.

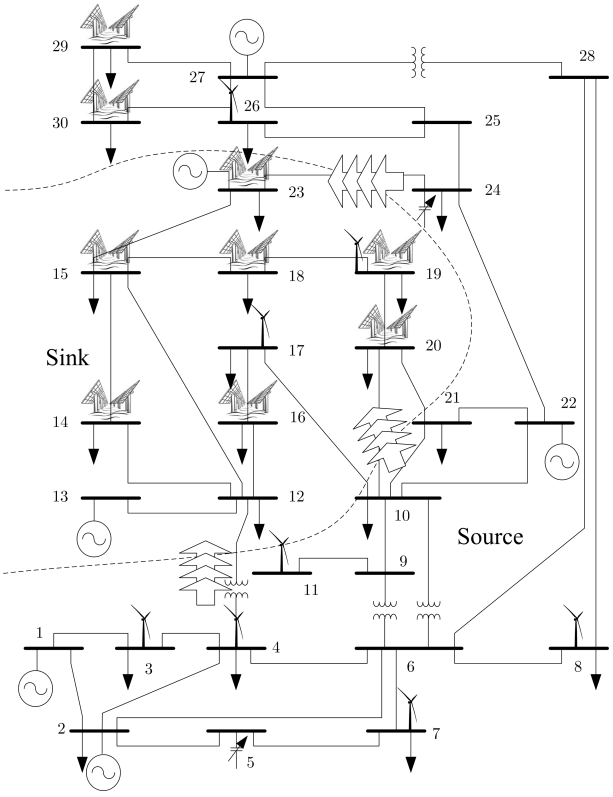

Fig. 8. Modified IEEE 30-bus system with wind and PV power generations.

D. Simulation Results

Due to the limit of the space, depicted in Fig. 9, only the PDF's of the MTC of Case 1 and Case 3c are presented for the illustration and discussion. It can be seen from Fig. 9 that without the uncertainty, except those from some outage cases, almost all MTC's lie at the base-case value of 142.6 MW. The TTC selected at the 10% risk is found to be 130.8 MW as indicated by a dashed line. In contrast, when considering the uncertainty of the forecast parameters, the shape of the PDF significantly changes, reflecting a stochastic nature of the MTC. The TTC selected at the 10% risk is found to be 127.4 MW, 3.4 MW smaller than that of Case 1. The results of the other cases also follow this characteristic. According to the results, it can be inferred that the presence of the uncertainty results in the smaller TTC.

Tabulated in Table II are the TTC's and monetary losses of all 7 study cases. They are also plotted in Fig. 10. It is found that the TTC tends to decrease as the uncertainty degree increases. To give an example, the TTC decreases from 130.8 MW to 128.0 MW as the uncertainty degree of the forecast generation outputs from renewable energy resources increases from 0% (Case 1) to 50% (Case 2c). In addition, the impact of the forecast demand uncertainty can be observed by comparing the TTC's of Case 2a, 2b, and 2c with those of Case 3a, 3b, and 3c respectively. The uncertainty of the forecast demand further reduces the TTC as the results prove.

The next point to be discussed is the interpretation of the risk and the monetary loss. The results listed in Table II show that the monetary loss depends on the value of the TTC. The

TABLE II
SUMMARY OF THE TTC'S AND MONETARY LOSSES AT 10% RISK

Case	TTC (MW)	Monetary loss ($/hr)
1	130.8	2036
2a	129.4	1987
2b	128.8	1974
2c	128.0	1954
3a	128.8	1957
3b	128.3	1949
3c	127.4	1931

TABLE III
SUMMARY OF THE ACTUAL RISKS AND MONETARY LOSSES

Case	Actual risk (%)	Actual monetary loss ($/hr)
2a	10.72	2060
2b	10.96	2082
2c	11.30	2104
3a	10.90	2063
3b	11.34	2087
3c	11.84	2115

larger the TTC, the larger the monetary loss. Interestingly, the monetary loss can be used to evaluate the impact of the uncertainty. Suppose that the system operator or the transmission system provider simply neglects such uncertainty. The TTC at 10% risk will be set to 130.8 MW (the TTC of Case 1). Nonetheless, when considering the uncertainty, the selected TTC at 130.8 MW results in the actual risk higher than 10%. The actual monetary loss also becomes larger than supposed. Consider Case 3c as an example, when the TTC is set to 130.8 MW, the risk and monetary loss increase to 11.84% and 2115$/hr respectively. This is analogous to moving the dashed line in the bottom plot of Fig. 9 slightly to the right. This phenomenon is depicted in Fig. 11 together with the data listed in Table III.

Another important aspect which can be observed from the obtained results is that the impact of the uncertainty is more clearly seen at the high risk level than at the low risk level. The top plot of Fig. 12 depicts the TTC's at 3 different risk levels; 10%, 15%, and 20%. They all decrease as the uncertainty degree increases as discussed previously. Setting the TTC of

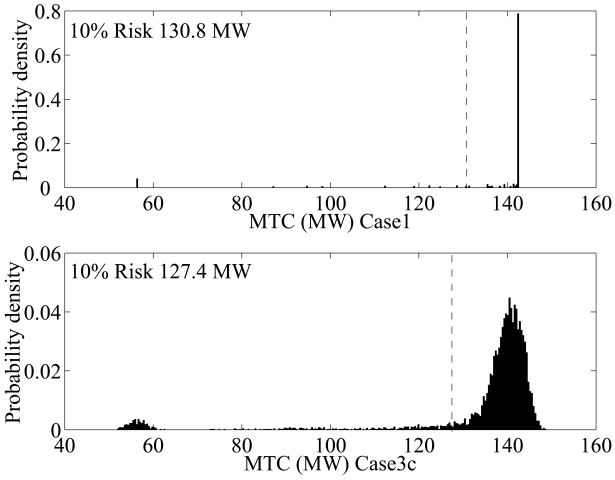

Fig. 9. PDF's of the MTC.

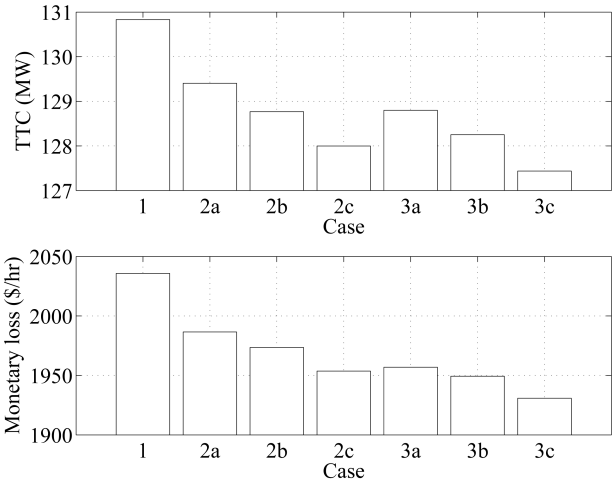

Fig. 10. TTC's selected at 10% risk and associated monetary losses.

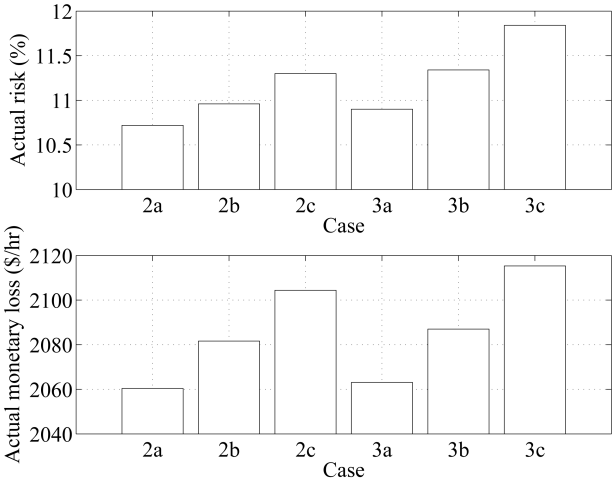

Fig. 11. Actual risks and monetary losses.

TABLE IV
SUMMARY OF THE TTC'S AT DIFFERENT RISK LEVELS

Case	TTC (MW)		
	10%	15%	20%
1	130.8	138.3	142.0
2a	129.4	136.6	138.7
2b	128.8	135.5	137.5
2c	128.0	134.5	136.3
3a	128.8	135.8	137.7
3b	128.3	134.7	136.7
3c	127.4	133.6	135.7

Case 1 as a benchmark for comparison, the reduction of the TTC due to the uncertainty is evaluated by the difference between the TTC of the interested case and that of Case 1. The TTC reductions of all 6 cases at 3 different risk levels are shown in the bottom plot of Fig. 12. The plot shows that among 3 different risk levels, the TTC reduction at 20% risk is the most negative. This can be explained from the PDF of MTC where the TTC is selected. Referring to the PDF of the MTC of Case 3c in Fig. 9, when the risk is high, the dashed line moves further to the right where a number of MTC samples are densely located. Note that some of these

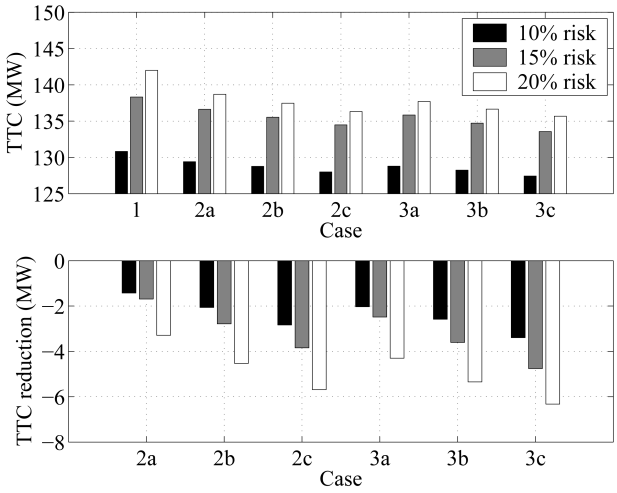

Fig. 12. TTC's and TTC reductions at 3 different risk levels.

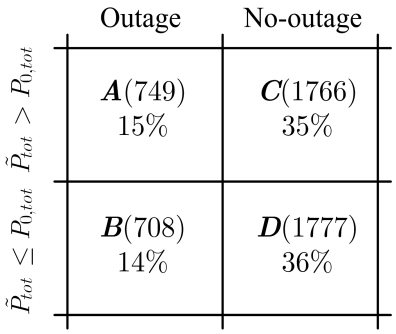

Fig. 13. Classification of the system cases.

MTC samples used to lie at the base-case value or its vicinity (the PDF of the MTC of Case 1). When the uncertainty is introduced, they begin to scatter. These scattering MTC samples can fall into the risk area if the specified risk is high. Consequently, the accumulated probability or the area of these MTC samples causes the TTC to become smaller.

E. Performance and Accuracy of the Partition Technique

This subsection examines the performance and accuracy of the proposed partitioned Monte Carlo simulation. The main contribution of this technique is the speed enhancement. The simulation using a different partitioned set results in different computational time. The more samples evaluated, the longer the computational time required.

From the total samples of 5000, 1457 are outage cases, and 2515 are the cases with the total sampled demand larger than the total base-case demand. The system cases are partitioned as shown in Fig. 13.

For an illustration of the TTC calculation with the partitioned Monte Carlo simulation, take Case 2c and Case 3c as an example. The risk is specified at 10%. The TTC and the computational time calculated using the full sample set, i.e. $A \cup B \cup C \cup D$, and the partitioned sets, i.e. $A \cup B$ and $A \cup B \cup C$ are summarized in Table V and VI. Since the TTC values obtained from the two partitioned sets have

TABLE V
RESULTS OF CASE 2C WITH DIFFERENT EVALUATED SETS

Evaluated set	TTC (MW)	CPU time (hr)	Error (%)
$A \cup B \cup C \cup D$	127.9976	1.6917	–
$A \cup B$	128.0816	0.7866	0.0656
$A \cup B \cup C$	128.0789	1.2229	0.0635

TABLE VI
RESULTS OF CASE 3C WITH DIFFERENT EVALUATED SETS

Evaluated set	TTC (MW)	CPU time (hr)	Error (%)
$A \cup B \cup C \cup D$	127.4358	1.7058	–
$A \cup B$	127.5407	0.7881	0.0823
$A \cup B \cup C$	127.5372	1.2360	0.0796

TABLE VII
COMPARISON OF THE ACCURACY AT DIFFERENT RISK LEVELS

Risk (%)	$\mathrm{TTC}_{A \cup B \cup C \cup D}$ (MW)	$\mathrm{TTC}_{A \cup B}$ (MW)	Error (%)
10	127.4358	127.5407	0.0823
15	133.5647	135.0400	1.1046
20	135.6788	138.5467	2.1137

only a slight difference, they are written in 4 decimals here for a clear comparison of their associated errors. Results from Table V and VI show that the computational time is significantly reduced with the use of the partitioned set. For instance, when using a set $A \cup B$, the computational time can be reduced as much as 50%. Nevertheless, there is some error since some of the MTC's within the risk region belongs to some other partitioned sets, e.g. a set C or D. As a result, the TTC calculated using the partitioned set is slightly larger than the actual value. To improve the accuracy, more samples should be evaluated. With the inclusion of a set C, the error reduces; however, requires longer computational time.

Interestingly, if the specified risk is low, using only a partitioned set $A \cup B$ may be sufficient to obtain an accurate result. This is due to the fact that, at low risk level, the risk region mainly consists of the MTC's from the partitioned set $A \cup B$. On the other hand, if the specified risk is high, the error increases. To examine this phenomenon, the comparison of the error of Case 3c using a partitoned set $A \cup B$ at different risk levels is summarized in Table VII.

VII. CONCLUSIONS

Through the use of Monte Carlo simulation and the proposed modeling of the generation from renewable energy resources, wind and PV power generation systems, the impact of the uncertainty on the TTC can be examined through the risk-based TTC values and associated monetary losses. Although the Monte Carlo simulation is powerful in recognizing and coping with uncertainty, it is time-consuming. The computational speed can be improved by using the proposed partition technique, making it still an attractive tool for the TTC calculation.

APPENDIX

The induction generator parameters are: Rated power $= 1.7$ MW, $R_s = 0.048$ p.u., $R_r = 0.0018$ p.u., $X_s = 0.0075$ p.u., $X_r = 0.12$ p.u., and $X_m = 3.8$ p.u..

REFERENCES

[1] Japan Renewable Energy Policy Platform Launched Toward 2050 [Online]. Available: www.japanfs.org/en/pages/028554.html.

[2] Milano, F, "Assessing Adequate Voltage Stability Analysis Tools for Networks with High Wind Power Penetration," *DRPT International Conference on Electric Utility Deregulation and Restructuring and Power Technologies*, pp. 2492−2497, April 2008.

[3] Ramezani, M. and Haghifam, M.R., "Modeling and Evaluation of Wind Turbines on Total Transfer Capability," *IEEE Power Engineering Society General Meeting, 2007*, pp. 1−6, June 2007.

[4] Wang Xinggang, Sun Wei, and Wang Chengshan, "Total Transfer Capability in Power System Including Large-Scale Wind Farms," *IEEE Region 10 Conference*, pp. 1−4, November 2006.

[5] Nattawut Paensuwan and Akihiko Yokoyama, "Risk-Based TTC Calculation in a Power System with Wind Generation Systems," *ISSE International Conference on Sustainable Energy 2008*, December 2008.

[6] A. E. Feijdoo and J. Cidras, "Modeling of Wind Farms in the Load Flow Analysis," *IEEE Trans. on Power Systems*, vol. 15, no.1, pp. 110−115, February 2000.

[7] Conti, S., Raiti, S., and Di Gregorio, C., "Probabilistic Load Flow for Distribution Networks with Photovoltaic Generators Part 2: Application to a Case Study," *ICCEP International Conference on Clean Electric Power*, pp. 137−141, May 2007.

[8] Transmission Transfer Capability Task Force, "Available Transfer Capability Definitions and Determination," North American Reliability Council, Princeton, NJ, June 1996.

[9] Rong-fu Sun, Yue Fan, Yong-hua Song, and Yuan-zhang Sun, "Development and Application of Software for ATC Calculation," *PowerCon 2006, International Conference on Power System Technology, 2006*, pp. 1−5, October 2006.

[10] Liang Min, and Abur, A., "Total Transfer Capability Computation for Multi-Area Power Systems," *IEEE Trans. on Power Systems*, vol. 21, no. 3, pp. 1141−1147, August 2006.

[11] Kulyos Audomvongseree and Akihiko Yokoyama, "Application of AC Equivalent to Total Transfer Capability Evaluation Using Two-Step Method," *Proc. PowerCon 2002, International Conference on Power System Technology*, vol. 1, pp. 383−387, October 2002.

[12] Ou, Y. and Singh, C., "Assessment of Available Transfer Capability and Margins," *IEEE Trans. on Power Systems*, vol. 22, no. 5, pp. 463−468, May 2002.

[13] Kulyos Audomvongseree and Akihiko Yokoyama, "Consideration of an Appropriate TTC by Probabilistic Approach," *IEEE Trans. on Power Systems*, vol. 19, no. 1, pp. 375−383, February 2004.

[14] Kulyos Audomvongseree and Akihiko Yokoyama, "Risk Based TTC Evaluation by Probabilistic Method," *Proc. PowerTech Conference 2003*, vol. 2, June 2003.

[15] M. Godoy Simões, and Felix A. Farret, *Renewable Energy Systems Design and Analysis with Induction Generators*. New York: CRC Press, 2004.

[16] Mukund R. Patel, *Wind and Solar Power Systems*. New York: CRC Press, 1999.

[17] L. Goel and R. Billinton, "A Procedure for Evaluating Interrupted Energy Assessment Rates in an Overall Electric Power System," *IEEE Trans. on Power Systems*, vol. 6, pp. 1390−1403, August 1991.

[18] Roy Billinton and Wenyuan Li, *Reliability Assessment of Electric Power Systems Using Monte Carlo Methods*. New York: Plenum, 1994.

Nattawut Paensuwan was born in Samutsakhon, Thailand, on May 26, 1982. He received the B.S. and M.S. from Chulalongkorn University, Bangkok, Thailand in 2004 and 2006 respectively. He is currently pursuing the Ph.D. degree at the University of Tokyo, Tokyo Japan under the MEXT scholarship. His research interests include power system deregulation, power system reliability evaluation, and renewable energy resources. He is a student member of IEEJ.

Akihiko Yokoyama (M'78) was born in Osaka, Japan, on October 9, 1956. He received the B.S., M.S., and Dr. Eng. degrees from the University of Tokyo, Tokyo, Japan, in 1979, 1981, and 1984, respectively. He has been with Department of Electrical Engineering, the University of Tokyo, since 1984 and currently is a professor in charge of power system engineering. He is a member of IEEJ, IEEE, and CIGRE.